Numerical of Thermo-hydro- mechanical modeling of CO_2 fracturing by the phase field approach

Vahid Ziaei-Rad[a], Mostafa Mollaali[b], Yongxing Shen[b,*]

[a] *Department of Civil Engineering, Isfahan University of Technology, Isfahan 84156-83111, Iran*
[b] *University of Michigan – Shanghai Jiao Tong University Joint Institute, Shanghai Jiao Tong University, Shanghai, China*

Abstract

Keywords: CO_2 fracturing, CO_2 fluid flow, phase field
2010 MSC: 65K10

1. Introduction

The objective of the paper at hand is to propose a phase field model to investigate the effect of thermo-hydro-mechanical CO_2 fracturing in saturated porous media.

2. Mathematical model

2.1. Porous medium deformation and fracture propagation

In this section, we briefly recapitulate the basic notations and the underlying equations of the phase field method for pressurized fractures in brittle materials.

2.1.1. Variational formulation of brittle fracture

Let $\Omega \subset \mathbb{R}^\eta$, $\eta = 2, 3$ be an open Lipchitz domain occupied by a porous medium with a lower-dimensional fracture $\mathcal{C} \in \mathbb{R}^{\eta-1}$, see Figure 1. Let the displacement field be $\boldsymbol{u} : \Omega \to \mathbb{R}^\eta$. Let $\Gamma_D, \Gamma_N \subseteq \partial\Omega$ be such that $\Gamma_D \cup \Gamma_N = \partial\Omega$ and $\Gamma_D \cap \Gamma_N = \emptyset$. Further, let $\boldsymbol{u}_D : \Gamma_D \to \mathbb{R}^2$ and $\boldsymbol{t}_N : \Gamma_N \to \mathbb{R}^2$ be prescribed displacement and traction boundary conditions, respectively. We denote by Γ_B the boundary of a borehole, and by $Q_f : \Gamma_B \to \mathbb{R}$ the fluid source. We have $\Gamma_P = \partial\Omega \setminus \Gamma_B$, and let $p_D : \Gamma_p \to \mathbb{R}$ be prescribed pressure. Also, $\mathbf{b} : \Omega \to \mathbb{R}^\eta$ is the body force per unit volume exerted to the solid.

We also need to define prescribed boundary condition for T. COMMENT

*Corresponding author
Email address: yongxing.shen@sjtu.edu.cn (Yongxing Shen)

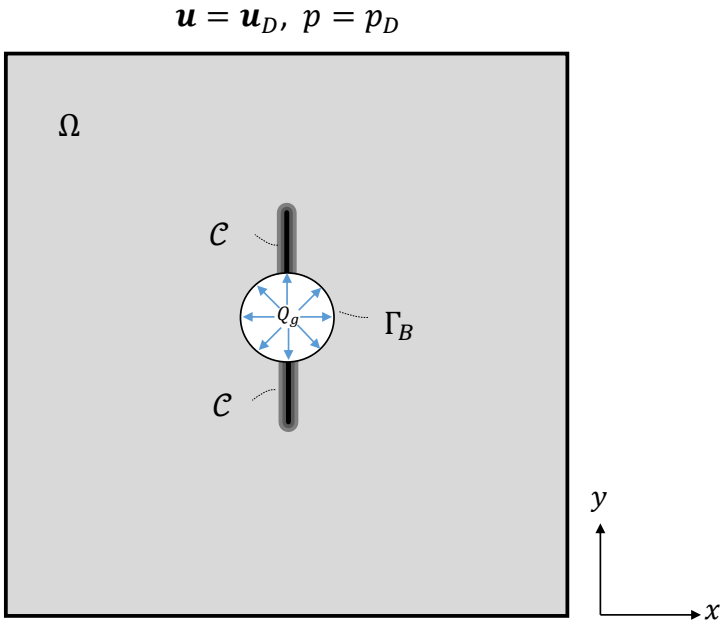

Figure 1: A bounded reservoir domain Ω with a lower-dimensional crack $\mathcal{C} \in \mathbb{R}^{\eta-1}$ (left) and its diffuse approximation.

The linearized strain tensor takes the form:

$$\boldsymbol{\varepsilon}(\boldsymbol{u}) = \frac{1}{2}(\nabla \boldsymbol{u} + \nabla \boldsymbol{u}^T) \tag{1}$$

which can be decomposed into two parts:

$$\boldsymbol{\varepsilon}(\boldsymbol{u}) = \boldsymbol{\varepsilon}_e + \boldsymbol{\varepsilon}_\theta. \tag{2}$$

Here, $\boldsymbol{\varepsilon}_e$ and $\boldsymbol{\varepsilon}_T$ are the elastic and thermal strain tensors, respectively. We assume that $\boldsymbol{\varepsilon}_\theta$ is proportional to the temperature θ via:

$$\boldsymbol{\varepsilon}_\theta = \beta(\theta - \theta_0)\mathbf{1}, \tag{3}$$

where θ_0 is a reference temperature, β is the linear expansion coefficient of the material, and $\mathbf{1}$ is the second-order identity tensor.

The energy of a poroelastic medium Ω with a crack $\mathcal{C}$ reads:

$$E(\boldsymbol{u}, \mathcal{C}) := \frac{1}{2}\int_{\Omega\setminus\mathcal{C}} \mathbb{C}\left(\boldsymbol{\varepsilon}_e(\boldsymbol{u}) - \frac{\alpha}{3K}p\mathbf{1}\right) : \left(\boldsymbol{\varepsilon}_e(\boldsymbol{u}) - \frac{\alpha}{3K}p\mathbf{1}\right) d\Omega - W(\boldsymbol{u}), \tag{4}$$

where $\mathbb{C} \in \mathbb{R}^4$ denotes the fourth-order Gassman tensor, and $\alpha \in [0, 1]$ and p are the Biot's coefficient and the pore pressure, respectively. Also, $K =$

$E/[3(1-2\nu)]$ where E, ν are Young's modulus and Poisson's ratio, respectively. The external work $W(\boldsymbol{u})$ is defined as:

$$W(\boldsymbol{u}) := \int_{\Omega} \boldsymbol{b} \cdot \boldsymbol{u} \, d\Omega + \int_{\Gamma_N} \boldsymbol{t}_N \cdot \boldsymbol{u} \, d\Gamma - \int_{\mathcal{C}} p\boldsymbol{n} \cdot [\boldsymbol{u}] \, d\Gamma, \tag{5}$$

where $\boldsymbol{n} \cdot [\boldsymbol{u}] \geq 0$ represents the displacement discontinuity on the fracture surface so that the term $\int_{\mathcal{C}} p\boldsymbol{n} \cdot [\boldsymbol{u}] \, d\Gamma$ is the work done by the absorbed fluid on the fracture surface.

The variational approach to fracture first proposed by Francfort and Marigo [1] defines the total energy as the sum of the potential energy and the surface energy required to create a fracture set $\mathcal{C}$. Let $\mathcal{H}^{\eta-1}(\mathcal{C})$ denote the lower-dimensional Hausdorff measure of $\mathcal{C}$. Taking the constant $G_c \in \mathbb{R}^+$ as the strain energy released per unit length of fracture extension, the total energy will be formed as:

$$\Pi[\boldsymbol{u}, \mathcal{C}] = E(\boldsymbol{u}, \mathcal{C}) + G_c \mathcal{H}^{\eta-1}(\mathcal{C}). \tag{6}$$

In the variational setting, the Griffith criteria will be the minimum of the total energy (6) with respect to any admissible displacement field $\boldsymbol{u}$ and any fracture set $\mathcal{C}$ subject to an irreversibility condition, i.e., the crack can never heal.

2.1.2. Regularized variational formulation of brittle fracture

To develop a numerical method to approximate (6), we need to replace the sharp description of crack $\mathcal{C}$ with a phase field representative, where the phase field is denoted as $d : \Omega \to [0, 1]$. Following the approach presented by Ambrosio and Tortorelli [2, 3], one can approximate $\mathcal{H}^{\eta-1}(\mathcal{C})$ with the help of an elliptic functional as:

$$\mathcal{C}_\ell[d] := \frac{1}{4c_\omega} \int_{\Omega} \left(\frac{\omega(d)}{\ell} + \ell \nabla d \cdot \nabla d \right) d\Omega, \tag{7}$$

In particular, regions with $d = 0$ and $d = 1$ correspond to the intact and fully broken materials, respectively. We denote by $\ell > 0$ the regularization length scale, which may also be interpreted as a material property, e.g., the size of the process zone. In (7), we consider $c_\omega = \int_0^1 \sqrt{\omega(d)}$ as a normalization constant such that as $\ell \to 0$, $\mathcal{C}_\ell[d]$ converges to the length of sharp crack $\mathcal{H}^{\eta-1}(\mathcal{C})$. Also, we choose $\omega(d) = d^2$, see [4, 5] for more elaborations.

The solid endures partial loss of stiffness due to the presence of fractures. To model this effect, the poroelastic energy needs to be degraded with respect to the evolution of the phase field. Also note that as the damaged material responds differently to tension and compression, we should let only a part of the poroelastic energy be degraded. Following [6], we assume that both volumetric expansion and deviatoric deformation contribute to crack propagation but not volumetric compression. A decomposition of $\boldsymbol{\varepsilon}_e$ into volumetric and deviatoric components reads:

$$\operatorname{vol} \boldsymbol{\varepsilon}_e := \frac{1}{3} (\operatorname{tr} \boldsymbol{\varepsilon}_e) \mathbf{1}, \quad \operatorname{dev} \boldsymbol{\varepsilon}_e := \boldsymbol{\varepsilon}_e - \operatorname{vol} \boldsymbol{\varepsilon}_e, \tag{8}$$

where $\mathrm{vol}\,\boldsymbol{\varepsilon}_e$ will also be decomposed into expansion and compression parts such that

$$\mathrm{vol}\,\boldsymbol{\varepsilon}_e = \mathrm{vol}_+\,\boldsymbol{\varepsilon}_e + \mathrm{vol}_-\,\boldsymbol{\varepsilon}_e, \quad \mathrm{vol}_\pm\,\boldsymbol{\varepsilon}_e = \frac{1}{\eta}\langle \mathrm{tr}\,\boldsymbol{\varepsilon}_e\rangle_\pm \mathbf{1}, \tag{9}$$

where $\langle a\rangle_\pm := (|a| \pm a)/2$ for all $a \in \mathbb{R}$. On this basis, we rewrite (4) with decomposition of the poroelastic energy into expansion/compression volumetric and deviatoric parts as:

$$\begin{aligned} E(\boldsymbol{u}, \mathcal{C}) := \frac{1}{2}\int_{\Omega\setminus\mathcal{C}} \mathbb{C}\Big\langle \mathrm{vol}\,\boldsymbol{\varepsilon}_e - \frac{\alpha}{3K}p\mathbf{1}\Big\rangle_+ : \Big\langle \mathrm{vol}\,\boldsymbol{\varepsilon}_e - \frac{\alpha}{3K}p\mathbf{1}\Big\rangle_+ \, d\Omega \\ + \frac{1}{2}\int_{\Omega\setminus\mathcal{C}} \mathbb{C}\Big\langle \mathrm{vol}\,\boldsymbol{\varepsilon}_e - \frac{\alpha}{3K}p\mathbf{1}\Big\rangle_- : \Big\langle \mathrm{vol}\,\boldsymbol{\varepsilon}_e - \frac{\alpha}{3K}p\mathbf{1}\Big\rangle_- \, d\Omega \\ + \int_{\Omega\setminus\mathcal{C}} \mathbb{C}\,\mathrm{dev}\,\boldsymbol{\varepsilon}_e : \mathrm{dev}\,\boldsymbol{\varepsilon}_e \, d\Omega - W(\boldsymbol{u}), \end{aligned}$$

To take into account any pre-existing crack, we define $\Gamma_d \subset \overline{\Omega}$ to be a set with Hausdorff dimension $\eta - 1$, and $d_0 : \Gamma_d \to [0, 1]$ as the Dirichlet boundary condition for d. Thus, we define the affine space of the admissible $\boldsymbol{u}$ and d fields:

$$\begin{aligned} \mathcal{S}_u &:= \left\{ \boldsymbol{u} \in H^1(\Omega; \mathbb{R}^\eta) \middle| \boldsymbol{u} = \boldsymbol{u}_D \text{ on } \Gamma_D \right\}, \\ \mathcal{S}_d &:= \left\{ d \in H^1(\Omega) \middle| 0 \le d \le 1 \text{ a.e.}, d = d_0 \text{ on } \Gamma_d \right\}. \end{aligned} \tag{10}$$

On this basis, the regularized variational formulation for brittle fracture of the solid reads: Find $(\boldsymbol{u} \times d) \in \mathcal{S}_{\boldsymbol{u}} \times \mathcal{S}_d$ that minimizes the following total energy:

$$\begin{aligned} \Pi_\ell(\boldsymbol{u}, d) := \frac{1}{2}\int_{\Omega} \mathbb{C}\Big\langle (1-d)\,\mathrm{vol}\,\boldsymbol{\varepsilon}_e - \frac{\alpha}{3K}p\mathbf{1}\Big\rangle_+ : \Big\langle (1-d)\,\mathrm{vol}\,\boldsymbol{\varepsilon}_e - \frac{\alpha}{3K}p\mathbf{1}\Big\rangle_+ \, d\Omega \\ + \frac{1}{2}\int_{\Omega} \mathbb{C}\Big\langle \mathrm{vol}\,\boldsymbol{\varepsilon}_e - \frac{\alpha}{3K}p\mathbf{1}\Big\rangle_- : \Big\langle \mathrm{vol}\,\boldsymbol{\varepsilon}_e - \frac{\alpha}{3K}p\mathbf{1}\Big\rangle_- \, d\Omega \\ + \int_{\Omega} g(d)\mathbb{C}\,\mathrm{dev}\,\boldsymbol{\varepsilon}_e : \mathrm{dev}\,\boldsymbol{\varepsilon}_e \, d\Omega \\ + \frac{G_c}{4c_\omega}\int_{\Omega} \left(\frac{\omega(d)}{\ell} + \ell \nabla d \cdot \nabla d \right) d\Omega - W(\boldsymbol{u}), \end{aligned} \tag{11}$$

35 I should add appropriate description for $(1-d)$. COMMENT

where $g(d)$ is a degradation function that satisfies $g(0) = 1$, $g(1) = 0$, and $g'(d) < 0$. A usual choice is $g(d) = (1-d)^2$ [7]. Note that the requirement $g'(d) < 0$ comes from the underlying irreversibility condition (the fracture can never heal) in time:

$$\partial_t d \ge 0. \tag{12}$$

Consequently, modeling of fracture evolution problems leads to inequality constraints, and sometimes gives rise to a variational inequality formulation. Also,

note that in this regularized form, the external work in (5) is rewritten as:

$$W(\boldsymbol{u}) := \int_{\Omega} \boldsymbol{b} \cdot \boldsymbol{u}\, d\Omega + \int_{\Gamma_N} \boldsymbol{t}_N \cdot \boldsymbol{u}\, d\Gamma - \int_{\Omega} p\boldsymbol{u} \cdot \nabla d\, d\Omega,$$

where $\int_{\Omega} \boldsymbol{u} \cdot \nabla d\, d\Omega$ represents the fracture volume [8].

It can be shown that when $\ell \to 0$, the regularized formulation $\Gamma-$converges to that with explicit crack representation, i.e., when $\ell \to 0$, the solution to the minimization problem (11) Γ-converges to that of $d\Pi[\boldsymbol{u}, \mathcal{C}] = 0$, and also $\mathcal{C}_\ell[d]$ converges to $\mathcal{H}^{\eta-1}(\mathcal{C})$. See Bourdin *et al.* [1] for the proof of the static anti-plane case.

2.2. Carbon dioxide as a compressible fluid

Assume the porous medium is saturated by a single-phase fluid. We denote by ϕ the porosity of the porous medium (the fraction of volume occupied by the fluid), and by ρ_f, ρ_s the fluid and solid density, respectively. Note that in this paper, the subscripts s and f refer to solid and fluid phases, respectively. The mass balance for the fluid reads:

$$\partial_t (\phi \rho_f) + \nabla \cdot (\phi \rho_f \mathbf{v}_f) = 0 \qquad \text{in } \Omega, \tag{13}$$

and for the solid phase:

$$\partial_t ((1-\phi)\, \rho_s) + \nabla \cdot ((1-\phi)\, \rho_s \mathbf{v}_s) = 0 \qquad \text{in } \Omega. \tag{14}$$

In (13) and (14), $\mathbf{v}_f$ and $\mathbf{v}_s$ are respectively the absolute value of fluid and solid velocity in the bulk. Multiplying ~~(13) by $\frac{1}{\rho_f}$ and~~ (14) by $\frac{1}{\rho_s}$, we sum up (13) and (14) to obtain:

$$\begin{aligned} &\frac{\phi}{\rho_f}\partial_t \rho_f + \frac{1}{\rho_f}\nabla \cdot (\phi \rho_f \mathbf{v}_f) + \frac{1-\phi}{\rho_s}\partial_t \rho_s \\ &+ \frac{1}{\rho_s}\left[(1-\phi)\rho_s \nabla \cdot \mathbf{v}_s + \mathbf{v}_s \cdot \nabla\left((1-\phi)\rho_s\right)\right] = 0. \end{aligned}$$

By neglecting $\nabla\left((1-\phi)\, \rho_s\right)$, it reads:

$$\frac{\phi}{\rho_f}\partial_t \rho_f + \frac{1}{\rho_f}\nabla \cdot (\phi \rho_f \mathbf{v}_f) + \frac{1-\phi}{\rho_s}\partial_t \rho_s + (1-\phi)\nabla \cdot \mathbf{v}_s = 0. \tag{15}$$

We introduce an intermediate term $\nabla \cdot (\phi \rho_f \mathbf{v}_s)$ as follows:

$$\frac{1}{\rho_f}\nabla \cdot (\phi \rho_f \mathbf{v}_s) = \frac{1}{\rho_f}\left[\phi \rho_f \nabla \cdot \mathbf{v}_s + \mathbf{v}_s \cdot \nabla\left(\phi \rho_f\right)\right] \approx \phi \nabla \cdot \mathbf{v}_s,$$

Having this, we define $\nabla \cdot (\phi \rho_f \mathbf{v}_f)$ in (15) as:

$$\begin{aligned} \frac{1}{\rho_f}\nabla \cdot (\phi \rho_f \mathbf{v}_f) &= \frac{1}{\rho_f}\nabla \cdot (\phi \rho_f \mathbf{v}_f) - \frac{1}{\rho_f}\nabla \cdot (\phi \rho_f \mathbf{v}_s) + \phi \nabla \cdot \mathbf{v}_s \\ &= \frac{1}{\rho_f}\nabla \cdot \left[\phi \rho_f \left(\mathbf{v}_f - \mathbf{v}_s\right)\right] + \phi \nabla \cdot \mathbf{v}_s. \end{aligned} \tag{16}$$

By substituting (16) in (15), we obtain:

$$\frac{\phi}{\rho_f}\partial_t\rho_f + \frac{1-\phi}{\rho_s}\partial_t\rho_s + \nabla\cdot\mathbf{v}_s + \frac{1}{\rho_f}\nabla\cdot\left[\phi\rho_f\left(\mathbf{v}_f-\mathbf{v}_s\right)\right] = 0, \quad \text{in } \Omega. \tag{17}$$

The first term on the left hand side of (17) can be written as:

$$\frac{\phi}{\rho_f}\partial_t\rho_f = \frac{\phi}{\rho_f}\left[\frac{\partial\rho_f}{\partial p}\partial_t p + \frac{\partial\rho_f}{\partial T}\partial_t T\right] = \phi\left[\beta_p\partial_t p + \beta_T\partial_t T\right], \tag{18}$$

where $\beta_p = \rho_f\partial\rho_f/\partial p$, and $\beta_T = \rho_f\partial\rho_f/\partial T$.

Here, I should add more explanations for water. COMMENT

The second term on the left hand side of (17) reads [10]:

$$\frac{1-\phi}{\rho_s}\partial_t\rho_s = (\alpha-\phi)\frac{1}{K_s}\partial_t p - \beta_s(\alpha-\phi)\partial_t T - (1-\alpha)\nabla\cdot\mathbf{v}_s, \tag{19}$$

where K_s denotes the bulk modulus of the grain material, $\beta_s = \frac{1}{\rho_s}\frac{\partial\rho_s}{\partial T}$ is the thermal expansion coefficient for the solid, and T is the absolute temperature.

The third term on the left hand side of (17) (also the last term of (19)) can be written as follows [11]:

$$\nabla\cdot\mathbf{v}_s = \nabla\cdot\dot{\boldsymbol{u}} = \left(\dot{\nabla}\cdot\boldsymbol{u}\right) = \partial_t\left(\mathrm{vol}\,\boldsymbol{\varepsilon}_e\right). \tag{20}$$

The forth term on the left hand side of (17) can be written in the form of Darcy's law. This law indicates a linear relationship between the relative velocity of fluid to solid and the head pressure gradient:

$$\mathbf{q} = \phi\left(\mathbf{v}_f-\mathbf{v}_s\right) = -\frac{\kappa}{\mu}\nabla p, \tag{21}$$

where κ is the permeability of rock, and μ is the dynamic fluid viscosity. Note that we neglect the effect of gravity in Darcy's law.

By substituting ~~(18),~~ (19), (20), and (21) in (17), the governing equation for CO_2 flow is written as follows:

$$\begin{aligned}\left[\phi\beta_p + \frac{\alpha-\phi}{K_s}\right]\partial_t p + \left[\phi\beta_T - \beta_s(\alpha-\phi)\right]\partial_t T \\ +\alpha\partial_t(\mathrm{vol}\,\varepsilon) + \frac{1}{\rho_f}\nabla\cdot(\rho_f\mathbf{q}) = 0 \quad \text{in } \Omega, \\ \rho_f\boldsymbol{q}\cdot\mathbf{n} = - \quad \text{on } \Gamma_B, \\ p = p_D \quad \text{on } \Gamma_P.\end{aligned} \tag{22}$$

Change of permeability. As the crack initiates, the permeability of the solid matrix increases inside the crack. To incorporate this effect into our model, we correlate the permeability to phase field by:

$$\kappa(d) = \kappa_0 + d\,(\kappa_c - \kappa_0)\,, \tag{23}$$

where κ_0, κ_c are the permeability of the intact material and the crack, respectively. Hence, a change of permeability will be assumed between the intact porous medium ($d = 0$) and the crack ($d = 1$). In (23), $\kappa_c = w_c^2/12$ where w_c is the fracture width. Following [12], w_c in a 2D setting can be estimated at each quadrature point as:

$$w_c = \sqrt{\left[h_e\,(1+\varepsilon_{11})\,n_{c1}\right]^2 + \left[h_e\,(1+\varepsilon_{22})\,n_{c2}\right]^2},$$

where h_e denotes the mesh size, ε_{ii} are the components of strain tensor $\boldsymbol{\varepsilon}$, and $\boldsymbol{n}_c = \frac{\nabla d}{|\nabla d|} = n_{ci}\boldsymbol{e}_i$ is the normal vector to the crack path.

2.3. Energy balance equation

We assume that the solid and fluid phases are in a state of thermodynamic equilibrium, i.e., the temperature of both phases are equal at each point in the dual-phase system:

$$\theta_s = \theta_f = \theta. \tag{24}$$

Based on the principle of conservation of heat energy, the heat increase rate of a system equals to sum of the heat conduction and heat generation rate in an arbitrary fixed volume. Thus, applying the Fourier law of heat conduction, the energy balance equation for each phase of the dual-system reads:

$$\left[(c\rho)_{s,f}\frac{\partial\theta}{\partial t} + c_{s,f}\rho_{s,f}\mathbf{v}_{s,f}\cdot\nabla\theta - \nabla\cdot\left[k_{s,f}\nabla\theta\right]\right] = 0, \tag{25}$$

where denote by c the heat capacity, and by k the heat conductivity matrix. Multiplying (25) by its porosity for each phase, neglecting $\mathbf{v}_s$, and using Darcy's law for the fluid phase, the governing equation of heat transfer in the porous media can be written as:

$$\begin{aligned}(c\rho)_{\text{eff}}\frac{\partial\theta}{\partial t} + c_f\rho_f\mathbf{q}\cdot\nabla\theta - \nabla\cdot(k_{\text{eff}}\nabla\theta) = 0 \quad &\text{in } \Omega,\\ k_{\text{eff}}\nabla\theta\cdot\mathbf{n} = -Q_T \quad &\text{on } \Gamma_B,\\ \theta = \theta_D \quad &\text{on } \Gamma_T.\end{aligned} \tag{26}$$

We let:

$$(c\rho)_{\text{eff}} := \phi(c_f\rho_f) + (1-\phi)(c_s\rho_s), \qquad k_{eff} := \phi k_f + (1-\phi)k_s. \tag{27}$$

Note the second term of (27) implies the effect of fluid flow on the heat transfer, as a convection term.

2.4. Summary of governing equations

The governing equations for modeling the CO_2 fracturing are summarized as follow: for the porous medium deformation, the functional defined in (11) is minimized among $(\boldsymbol{u}, d) \in \mathcal{S}_u \times \mathcal{S}_d$ under the constraint (12), while for the compressible fluid the boundary value problem (22) is used to solve for the pressure p. Also, a governing equation of heat transfer is derived from (26).

3. Numerical solution

In this section we present an algorithm that adopts standard procedures to obtain a numerical method to solve the initial boundary value problem presented in Section 2. In this algorithm, a staggered approach is employed to solve the underlying equations, i.e., the solution is obtained via iteration between the variables [7, 1]. This idea is based on the fact that by fixing two variables, the problem becomes convex in the remaining unknown. However, one drawback for such an approach is that it might need many iterations to achieve convergence among the three fields.

For the problem at hand, we need to solve a coupled system consisting of mass balance for the compressible fluid and a dissipative potential energy with the phase field. We provide a fully iterative approach in which at each stage we solve for one unknown while the other two variables are fixed to their values at the last iteration. Readers are referred to Algorithm 1 for complete elaboration.

We implement our method on FEniCS, an open-source finite element software [15, pp. 173–225]. Therein, the user merely needs to provide the variational form of the problem as well as the geometry and mesh information. Then, a big advantage of FEniCS is that the software itself completes all steps toward generating the global stiffness matrix.

Below we show an excerpt of the used FEniCS code. This piece of code performs some calculations for line 6 in Algorithm 1 wherein $\boldsymbol{u}$ is solved for while the other two unknowns are fixed. It first defines $\boldsymbol{\varepsilon}$, ψ_0, and $\psi(\boldsymbol{\varepsilon}, d)$ in lines 1, 3, and 5, respectively. Then, the standard finite element shape functions are defined in line 8, and the admissible function space (`TrialFunction`), the test function space (`TestFunction`), and the unknown function $\boldsymbol{u}$ (`Function`) are defined in line 9. Afterwards, the elastic energy is introduced as a variational form in line 11. Finally, in lines 12 and 13, the code takes the first variation $\delta\Pi[(\boldsymbol{u}, d); \bar{\boldsymbol{u}}]$ (**??**) and the second variation $\delta^2\Pi[(\boldsymbol{u}, d); \bar{\boldsymbol{u}}; \delta\boldsymbol{u}]$ (A.2a) and builds the nodal residual vector as `Residual_u` and the tangent stiffness matrix as `Jacobian_u`.

```
1 def eps(u_):
2 return sym(grad(u_))
3 def psi_0(u_):
4 return 0.5 * lmbda * tr(eps(u_))**2 + mu * eps(u_)**2
5 def psi_(u_, d_):
6 return (1 - d_)**2 * psi_0(u_)
7
```

Algorithm 1: Algorithm for modeling the CO_2 by phase field.

Input: $\boldsymbol{u}_0$, d_0, p_0, ρ_0, T_0, and ε_{tol}

Output: $\boldsymbol{u}_n$, d_n, p_n, T_n, and $n = 1, \cdots, N$

Set mechanical, flow, and thermal boundary conditions σ_1, σ_3, Q_f, and Q_T;

for $n = 1$ *to* N*;* **do**

  Set $t = n\Delta t$ and $i = 0$; `/* i is an iteration counter */`

  $m = 0$; `/* m is another iteration counter */`

  repeat

    Step - U: compute $\boldsymbol{u}_n$ with (A.1a);

    Step - d: compute d_n with (A.1b);

    $i + 1 \leftarrow i$

  until $\left\|\boldsymbol{u}_n^{(i)} - \boldsymbol{u}_n^{(i-1)}\right\|_2 < \varepsilon_{tol}$ ***and*** $\left\|d_n^{(i)} - d_n^{(i-1)}\right\|_2 < \varepsilon_{tol}$;

  repeat

    Step - P: compute p_n with (A.3);

    Step - T: compute T_n with (A.4);

    Update $\rho_n^{(m+1)} \leftarrow \rho(p_n^{(m)})$ with (**??**);

    $m + 1 \leftarrow m$

  until $\left\|p_n^{(m)} - p_n^{(m-1)}\right\|_2 < \varepsilon_{tol}$ ***and*** $\left\|T_n^{(m)} - T_n^{(m-1)}\right\|_2 < \varepsilon_{tol}$;

  $\boldsymbol{u}_{n-1} \leftarrow \boldsymbol{u}_n$;

  $p_{n-1} \leftarrow p_n$;

  $\rho_{n-1} \leftarrow \rho_n$;

  $T_{n-1} \leftarrow T_n$;

end

```
V_u = VectorFunctionSpace(mesh, "CG", 1)
u_, u, u_t = Function(V_u), TrialFunction(V_u), TestFunction(V_u)

energy_elastic = psi_(u_, d_) * dx
Residual_u = derivative(energy_elastic, u, u_t)
Jacobian_u = derivative(Residual, u_, u_t)
```

To solve the three unknowns, we select for $\boldsymbol{u}$ and p the linear solver MUMPS which is convenient for solving large linear systems [16], and for d the TAO optimization solver integrated into the PETSc library [17, 18], which has the capability of solving inequality constrained optimization problems as the one at hand. Interested readers are referred to [19] for more information about the applied solvers.

AppendixA. Weak forms

Here we provide weak forms useful for FEniCS implementation.

AppendixA.1. Porous medium

To proceed, let the test function spaces be

$$\mathcal{V}_u := \left\{ \bar{\boldsymbol{u}} \in H^1\left(\Omega; \mathbb{R}^2\right) \middle| \bar{\boldsymbol{u}} = \boldsymbol{0} \text{ on } \Gamma_D \right\},$$
$$\mathcal{V}_d := H^1(\Omega).$$

Then we derive the first variations of the energy functional (11), which will be needed for stating the weak form:

$$\begin{aligned}
&\Pi_\ell\left[(\boldsymbol{u}, d); \bar{\boldsymbol{u}}\right] := \\
&\quad \int_\Omega \mathbb{C}\Big\langle (1-d)\,\mathrm{vol}[\boldsymbol{\varepsilon}_e(\boldsymbol{u})] - \frac{\alpha}{3K} p\mathbf{1} \Big\rangle_+ : \Big\langle (1-d)\,\mathrm{vol}[\boldsymbol{\varepsilon}_e(\bar{\boldsymbol{u}})] - \frac{\alpha}{3K} p\mathbf{1} \Big\rangle_+ \, d\Omega \\
&\quad + \int_\Omega \mathbb{C}\Big\langle \mathrm{vol}[\boldsymbol{\varepsilon}_e(\boldsymbol{u})] - \frac{\alpha}{3K} p\mathbf{1} \Big\rangle_- : \Big\langle \mathrm{vol}[\boldsymbol{\varepsilon}_e(\bar{\boldsymbol{u}})] - \frac{\alpha}{3K} p\mathbf{1} \Big\rangle_- \, d\Omega \\
&\quad + \int_\Omega g(d) \mathbb{C}\,\mathrm{dev}[\boldsymbol{\varepsilon}_e(\boldsymbol{u})] : \mathrm{dev}[\boldsymbol{\varepsilon}_e(\bar{\boldsymbol{u}})] \, d\Omega,
\end{aligned} \tag{A.1a}$$

$$\begin{aligned}
&\delta\Pi_\ell\left[(\boldsymbol{u}, d); \bar{d}\right] := \\
&\quad \int_\Omega \mathbb{C}\Big\langle (d-1)\,\mathrm{vol}[\boldsymbol{\varepsilon}_e(\boldsymbol{u})] - \frac{\alpha}{3K} p\mathbf{1} \Big\rangle_+ : \Big\langle \bar{d}\,\mathrm{vol}[\boldsymbol{\varepsilon}_e(\boldsymbol{u})] - \frac{\alpha}{3K} p\mathbf{1} \Big\rangle_+ \, d\Omega \\
&\quad + \int_\Omega g'(d)\bar{d}\; \mathbb{C}\,\mathrm{dev}[\boldsymbol{\varepsilon}_e(\boldsymbol{u})] : \mathrm{dev}[\boldsymbol{\varepsilon}_e(\boldsymbol{u})] \, d\Omega \\
&\quad + \frac{G_c}{4c_\omega} \int_\Omega \left(\frac{\omega'(d)\,\bar{d}}{\ell} + 2\ell \nabla d \cdot \nabla \bar{d} \right) d\Omega.
\end{aligned} \tag{A.1b}$$

The weak form can thus be stated as: Find $(\boldsymbol{u} \times d) \in \mathcal{S}_{\boldsymbol{u}} \times \mathcal{S}_d$, such that for all admissible functions $\left(\bar{\boldsymbol{u}} \times \bar{d}\right) \in \mathcal{V}_{\boldsymbol{u}} \times \mathcal{V}_d$, $\delta\Pi_\ell\left[(\boldsymbol{u}, d); \bar{\boldsymbol{u}}\right] = 0$ and $\delta\Pi_\ell\left[(\boldsymbol{u}, d); \bar{d}\right] = 0$.

Also we take another variation from (11) which will be needed for the discretized formulation:

I should check the second variations.

$$\delta^2\Pi_\ell\left[(\boldsymbol{u}, d); \bar{\boldsymbol{u}}, \delta\boldsymbol{u}\right] = \int_\Omega \boldsymbol{\varepsilon}(\delta\boldsymbol{u}) : \mathbb{C}[\boldsymbol{\varepsilon}(\boldsymbol{u}), d] : \boldsymbol{\varepsilon}(\bar{\boldsymbol{u}}) \, d\Omega, \tag{A.2a}$$

$$\begin{aligned}
\delta^2\Pi_\ell\left[(\boldsymbol{u}, d); \bar{d}, \delta d\right] &= \int_\Omega \delta d\; g''(d)\psi_+(\boldsymbol{\varepsilon})\bar{d}\, d\Omega \\
&\quad + \int_\Omega (\alpha - 1)\, g''(d)\bar{d}\; \delta d\, p\, \mathrm{div}\, \boldsymbol{u}\; d\Omega + \int_\Omega g''(d)\bar{d}\; \delta d\; \nabla p \cdot \boldsymbol{u}\; d\Omega \\
&\quad + \frac{G_c}{4c_w} \int_\Omega \left[\frac{\delta d\; w''(d)\bar{d}}{\ell} + 2\ell \nabla(\delta d) \cdot \nabla \bar{d} \right] d\Omega,
\end{aligned} \tag{A.2b}$$

where the fourth-order tensor $\mathbb{C}[\boldsymbol{\varepsilon}(\boldsymbol{u}), d] = \left.\frac{\partial \boldsymbol{\sigma}(\boldsymbol{\varepsilon}, d)}{\partial \boldsymbol{\varepsilon}}\right|_{\boldsymbol{\varepsilon} = \boldsymbol{\varepsilon}(\boldsymbol{u})}$ is the tangent elasticity tensor.

AppendixA.2. Compressible (CO_2) fluid flow discretization

The compressible fluid flow discretization is also done via the finite element method. We first discretize in time and then in space. We will adopt the backward Euler method for time discretization.

To proceed, let the admissible set of pressure be:

$$\mathcal{S}_p := \left\{ p \in H^1(\Omega) \middle| p = p_D \text{ on } \Gamma_P \right\}.$$

The test function space can be defined as:

$$\mathcal{V}_p = \left\{ \overline{p} \in H^1(\Omega) \middle| \overline{p} = 0 \text{ on } \Gamma_P \right\}.$$

The weak form can be stated as: find $p \in \mathcal{S}_p$ such that for all admissible functions $\overline{p} \in \mathcal{V}_p$,

$$\begin{aligned} &\frac{1}{\Delta t} \int_\Omega \frac{\alpha - \phi}{K_s} \left(p - p^{n-1} \right) \overline{p} \, d\Omega - \frac{1}{\Delta t} \int_\Omega \beta_s (\alpha - \phi) \left(T - T^{n-1} \right) \overline{p} \, d\Omega \\ &+ \frac{\alpha}{\Delta t} \int_\Omega (\mathrm{vol}\, \boldsymbol{\varepsilon}_e - (\mathrm{vol}\, \boldsymbol{\varepsilon}_e)^{n-1}) \overline{p} \, d\Omega + \int_\Omega \frac{\kappa}{\mu} \nabla p \cdot \nabla \overline{p} \, d\Omega - \int_{\Gamma_B} Q_p \overline{p} \, d\Gamma = 0, \end{aligned} \tag{A.3}$$

where p^{n-1}, T^{n-1}, and $(\mathrm{vol}\, \boldsymbol{\varepsilon}_e)^{n-1}$ are obtained from previous time step.

AppendixA.3. Energy balance

To proceed, let the admissible set of pressure be:

$$\mathcal{S}_T := \left\{ T \in H^1(\Omega) \middle| T = T_D \text{ on } \Gamma_T \right\}.$$

The test function space can be defined as:

$$\mathcal{V}_T = \left\{ \overline{T} \in H^1(\Omega) \middle| \overline{T} = 0 \text{ on } \Gamma_T \right\}.$$

The weak form can be stated as: find $T \in \mathcal{S}_T$ such that for all admissible functions $\overline{T} \in \mathcal{V}_T$:

$$\begin{aligned} &\frac{1}{\Delta t} \int_\Omega (c\rho)_{\text{eff}} \left(T - T^{n-1} \right) \overline{T} \, d\Omega + \int_\Omega \left(c_f \rho_f \mathbf{q} \cdot \nabla T \right) \overline{T} \, d\Omega \\ &- \int_\Omega k_{\text{eff}} \nabla T \cdot \nabla \overline{T} \, d\Omega - \int_{\Gamma_B} Q_T \overline{T} \, d\Gamma = 0 \end{aligned} \tag{A.4}$$

Acknowledgments

This work is supported by the National Natural Science Foundation of China with grant #11402146. YS also acknowledges the financial support by the Young 1000 Talent Program of China.

[1] B. Bourdin, G. A. Francfort, J. J. Marigo, The variational approach to fracture, Journal of Elasticity 91 (2008) 5–148.

[2] L. Ambrosio, V. M. Tortorelli, On the Approximation of Free Discontinuity Problems, Scuola Normale Superiore, 1990.

[3] L. Ambrosio, V. M. Tortorelli, On the approximation of functionals depending on jumps by quadratic, elliptic functionals, Bollettino dell'Unione Matematica Italiana 6 (1992) 105–123.

[4] E. Tanné, T. Li, B. Bourdin, J.-J. Marigo, C. Maurini, Crack nucleation in variational phase-field models of brittle fracture, Journal of the Mechanics and Physics of Solids 110 (2018) 80–99.

[5] B. Bourdin, J.-J. Marigo, C. Maurini, P. Sicsic, Morphogenesis and propagation of complex cracks induced by thermal shocks, Physical Review Letters 112 (2014) 014301.

[6] H. Amor, J.-J. Marigo, C. Maurini, Regularized formulation of the variational brittle fracture with unilateral contact: numerical experiments, Journal of the Mechanics and Physics of Solids 57 (8) (2009) 1209–1229.

[7] B. Bourdin, G. A. Francfort, J.-J. Marigo, Numerical experiments in revisited brittle fracture, Journal of the Mechanics and Physics of Solids 48 (4) (2000) 797–826.

[8] B. Bourdin, C. Chukwudozie, K. Yoshioka, A variational approach to the numerical simulation of hydraulic fracturing, in: M. Jirásek, O. Allix, N. Moës, J. Oliver (Eds.), Computational Modeling of Fracture and Failure of Materials and Structures: Proceedings of CFRAC 2013, 2013, p. 180.

[9] M. Mahmoud, Development of a new correlation of gas compressibility factor (z-factor) for high pressure gas reservoirs, Journal of Energy Resources Technology 136 (1) (2014) 012903.

[10] R. W. Lewis, B. A. Schrefler, The finite element method in the static and dynamic deformation and consolidation of porous media, Vol. 2, Wiley Chichester, 1998.

[11] A. Merxhani, An introduction to linear poroelasticity. arxiv preprint arxiv: 160704274 google scholar.

[12] Y. Heider, S. Reiche, P. Siebert, B. Markert, Modeling of hydraulic fracturing using a porous-media phase-field approach with reference to experimental data, Engineering Fracture Mechanics 202 (2018) 116–134.

[13] M. Sheng, G. Li, S. Shah, X. Jin, Extended finite element modeling of multi-scale flow in fractured shale gas reservoirs, Vol. 5, 2012.

[14] F. Civan, Effective correlation of apparent gas permeability in tight porous media, Transport in Porous Media 82 (2) (2010) 375–384.

[15] A. Logg, G. N. Wells, J. Hake, DOLFIN: A C++/Python Finite Element Library, Springer Berlin Heidelberg, Berlin, Heidelberg, 2012.

[16] P. R. Amestoy, I. S. Duff, J.-Y. L'Excellent, J. Koster, MUMPS: A general purpose distributed memory sparse solver, in: International Workshop on Applied Parallel Computing, Springer, 2000, pp. 121–130.

[17] T. Munson, J. Sarich, S. Wild, S. Benson, L. McInnes, Toolkit for advanced optimization (TAO) users manual, Tech. rep., Technical Report No. ANL/MCS-TM-322-Revision 3.5 (Argonne National Laboratory, 2014) (2014).

[18] S. Balay, S. Abhyankar, M. F. Adams, J. Brown, P. Brune, K. Buschelman, L. Dalcin, V. Eijkhout, W. D. Gropp, D. Kaushik, M. G. Knepley, D. A. May, L. C. McInnes, R. T. Mills, T. Munson, K. Rupp, P. Sanan, B. F. Smith, S. Zampini, H. Zhang, H. Zhang, PETSc users manual, Tech. Rep. ANL-95/11 - Revision 3.9, Argonne National Laboratory (2018).

[19] C. Bilgen, A. Kopaničáková, R. Krause, K. Weinberg, A phase-field approach to conchoidal fracture, Meccanica 53 (6) (2018) 1203–1219.